Image analysis used for aluminium alloy microstructure investigation

M. Krupiński [a,*], K. Labisz [a], L.A. Dobrzański [a], Z. Rdzawski [a,b]

[a] Division of Materials Processing Technology, Management and Computer Techniques
in Materials Science, Institute of Engineering Materials and Biomaterials,
Silesian University of Technology, ul. Konarskiego 18a, 44-100 Gliwice, Poland
[b] Institute of Non-Ferrous Metals, ul. Sowińskiego 5, 44-100 Gliwice, Poland
* Corresponding author: E-mail address: mariusz.krupinski@polsl.pl

Materials

ABSTRACT

Purpose: In this work the metallographic microstructure analysis of the investigated AlSi7Cu3Mg aluminium cast alloy was performed for samples cooled with different cooling rate settings. The preformed investigations are subjected to the analysis of cooling rate influence on the phase morphology.

Design/methodology/approach: The solidification process itself is analysed using the UMSA device by appliance of the Derivative Thermo Analysis. The influence of the cooling rate on the alloy microstructure was investigated using computer aided image analysis, in this work also the content of particular phases was analysed, as well the percentage of pinholes compared to the chosen cooling rate.

Findings: The treated sample is without holes, cracks and defects as well as has a slightly higher hardness value compared to the as-cast material.

Research limitations/implications: The investigated samples were made of the cylindrical shape and were cooled in the range of 0.2°C/s to 1.25°C/s. In this work also the derivative thermoanalysis was performed to determine the correlation between the chosen cooling rate and the microstructure as well changes in the derivative curve shape. For alloy cooling with chosen cooling rate as well for the derivative thermo-analysis the UMSA analysator was applied.

Practical implications: The investigated material can find its use in the foundry industry; an improvement of component quality depends mainly on better control over the production parameters.

Originality/value: The originality of this work is based on applying of regulated cooling rate of aluminium alloy for structure and mechanical properties changes. As an effect of this study it will be possible to understand and to influence the mechanism of structure forming, refinement and nucleation. Also a better understanding of the thermal characteristics will be provided to achieve a desirable phase morphology required for application of this material under production conditions.

Keywords: Metallic alloys; Thermo analysis; Phases morphology; Al-Si-Cu

1. Introduction

The crystallisation process occurs, in case of the cast metal alloys, after casting of the liquid metal into the mould. The parameters of this process determine the microstructure of the obtaining casts, which is critical for the achieved physical and mechanical properties [1].

As a result of the metal crystallisation in the mould there can be formed three different microstructure areas: in place of the metal-mould contact is formed the so called frozen crystals/grains area. This composition consist mainly of equiaxial, very small crystals with a random orientation, here occurs the fastest heat transport; -area with columnar shaped crystals/grains; this is an area with a middle cooling rate value; -area with equiaxial crystals/grains, which is present in the central part of the cast, this microstructure is characterised by a macroscopic isotropy and contains also crystals with a random orientation, with a bigger crystals size compared to those present in the frozen crystals area, here occurs the slowest cooling rate in the whole cast. The occurrence of these areas depends on several factors like: physical and chemical state of the liquid metal (chemical composition, distribution of inhibitors of the heterogenic nucleation), cooling rate of the cast (heat transport from the liquid metal), convection intensity of the liquid metal [2-4].

The microstructure of an engineering material depends on its properties. For the reason of the dependence settlement between the microstructure and properties there should be performed an image analysis. The process of image analysis can be defined as a image investigation for object identification and its contribution valuation on the properties. This process consist of data accusation from the image as well the analysis through: identification, classification, measurement and valuation of the physical state of the sample, analysis of the pattern observed in the image as well the spatial relation between the features of a given sample. In case of data acquisition about metal microstructure, the manual, stereological or conventional image analysis methods are often time-consuming and not always user friendly. As a solution for this problem there are applied computer aided qualitative and quantitative metal microstructure analysis [5-8].

For determination and calculation of the thermal processes parameters occurred during the solidification some thermodynamical calculation should be performed. A very important tool is the cooling rate curve with determined baseline. The baseline equation calculation requires that the thermal system being considered (i.e., the alloy sample and the cup) complies with Newtonian cooling model requirements. This means that the temperature within the system must be spatially uniform or, at least, that the temperature gradient in any direction within the system must be negligible at any instant during the cooling process [9].

The overall heat transmission coefficient is based on the total thermal resistance between the temperature of the solidifying sample (T_c) and the environment temperature (T_∞).

Under the assumption described, the energy balance can be written as follows:

$$\rho C_\rho V \frac{d(T_c - T_\infty)}{dT} = -UA(T_c - T_\infty) + \frac{dQ_L}{dt} \qquad (1)$$

In case were no metallurgical reaction occurs (i.e., when Q_L=0) Equation 1 can be reduced to another form, where the baseline equation can be set:

$$\frac{dT_c}{dt} = \left(-\frac{UA}{\rho C_\rho V}\right)(T_c - T_\infty) \qquad (2)$$

where:
Q_L - Crystallisation heat,
Cp - Heat capacity,
U – heat transmission coefficient,
dT_c/dt - Differential,
dt, T_O Environment temperature,
T_c – Solidifying temperature,
$\rho C_\rho V$ – Heat capacity term.

However, since this new alloy was recently engineered, the solidification kinetics and the sequence of the phase transformations in relation to the as-cast and heat-treated structures needs to be further understood, quantified and implemented for further improvement of the casting technology and cast component service characteristics. Moreover, the optimum conditions for liquid metal treatment must be understood to gain full benefit from the achievable refinement of the primary Si particles. The cooling rate is proportional to the heat extraction from the sample during solidification. Due to the increase the cooling rate the nucleation undercooling increase. The phenomenon of an increase in the nucleation temperature with an increase in the solidification rate depends on the mobility of the clusters of atoms in the melt. These groups of the froze atoms produces the fluctuation clusters and fluctuation embryos, which are the nucleation primers. The increase of the cooling rate with an increase amount of the nucleation primers and reduction of the recalescence temperature is well established fact. This effect have influence on the grain size, and precipitation morphology and distribution [10-18].

The concept of this work include rapid and slow quenching rate experiments to monitor the solidification process mainly of the Al_2Cu an iron and magnesium containing phases. The goal of this paper is to present the structure changes mechanism on the basis of the characteristic of the Al-Si-Cu alloy, which is used for monolithic engine block widely in the automotive industry due to its good casting characteristics and mechanical properties [19, 20].

2. Material and experimental procedure

The aim of his work was the analysis of phases present on metallographic micrographs of a AlSi7Cu3Mg cast aluminium alloy (Table 1) cooled with different cooling rates. The investigations include a analysis of cooling rate influence on phase morphology. The influence of the cooling rate on the

alloy microstructure was investigated using computer image analysis, in this work also the amount of the present phases was analysed as well the analyses was performed of the pores percentage amount in comparison to the cooling rate. The analysis was performed on specially worked out image from polished samples using special software for image analysis. For this analysis ca. 300 images of metallographic samples was used.

Table 1.
Chemical composition of AC-AlSi7Cu3Mg aluminium alloy

Mass concentration of the element, in wt. %, AA standard		
Al	Cu	Mg
8.5-8	3-4	0.3-0.6
Mn	Fe	Ti
0.2-0.65	≤ 0.8	≤ 0.25
Zn		Ni
≤ 0.65		≤ 0.3

The images of metallographic microstructures was obtaining as a result of thermo-derivative analysis, the samples for investigations were of the following shape:
- cylindrical (Fig. 1A), cooling rate: 0.2°C/s, 0.5°C/s, 1°C/s,
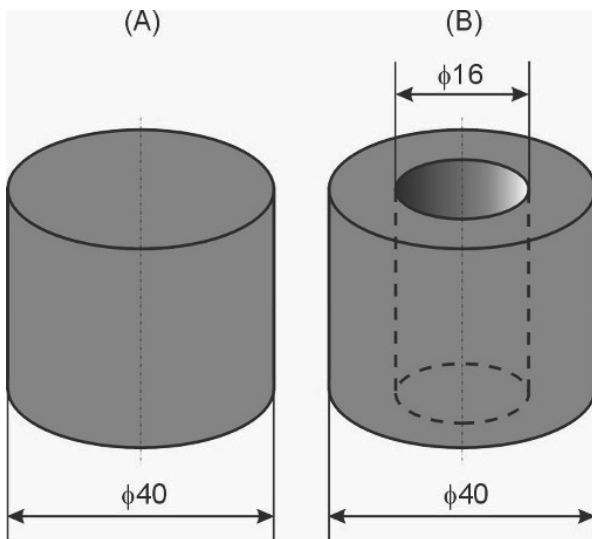- hollow-cylindrical (Fig. 1B), cooling rate 1.25°C/s.

Fig. 1. Dimensions of the cylindrical sample types used for investigations

For statement of the interdependence between the chemical composition and the structure of the AC-AlSi7Cu3Mg (EN 1706:2001) aluminium cast alloy (Table 1), cooled with different cooling speed, followed investigations were made:
- Alloy structure using Leica MEF4A optical microscope together with the image analysis software. The samples for optical microscope investigations were electro etched using 30% HBF_4 solution with proper direct current conditions as well in the 5% HF solution;

- chemical composition of the Al alloy using qualitative and quantitative X-Ray analysis, as well EDS microanalysis;
- derivative thermo analysis using the UMSA thermo simulator, with a computer-controlled cooling system. This is necessary for precise simulation of the cooling conditions like temperature and time during the crystallization of the investigated alloy.

Analysis of metallographic microstructure image was performer in a following way:
1) Colour segmentation for a chosen phase,
2) Binarising of a given phase,
3) Phase segmentation. Matrix generating for give phases, quantitative analysis. For each phase the matrix is created separately, for the reason of a non uniform colour of each phase, by the following parameters:
   - Sensitivity of the colour sampling, the higher numerical value the lower tolerance for halftone and other colours;
   - Sample size 1x1 for small phases as well 3x3 for big phases;
4) In percent content of the present phases.

3. Research results and discussion

In this work there was analysed the influence of the cooling speed in the range of 0.2°-1.25°C/s on microstructure of the AlSi7Cu3Mg cast aluminium alloys. Some micrographs of the microstructure were showed in Figs. 2-9. In Fig. 10 are shown the phases, which were analysed in the work. In Fig. 11 the image analysis was presented of the $Al_{15}(MnFe)_3Si_2$ phase for identification in the microstructure image and following quantitative analysis. It is possible on the basis of the performed measurements of the structure image to make some conclusions about the precipitation morphology changes. The results of the measurements for all images are analysed statistically.
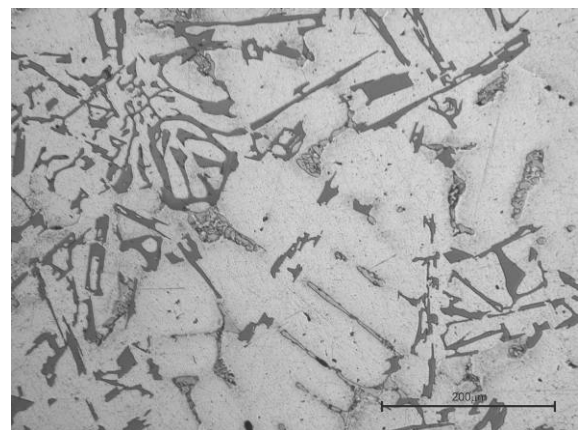

Fig. 2. Optical micrograph of the Al alloy, cylindrical sample of the A type, cooling rate 0.2ºC/s, plane perpendicular to the sample axis
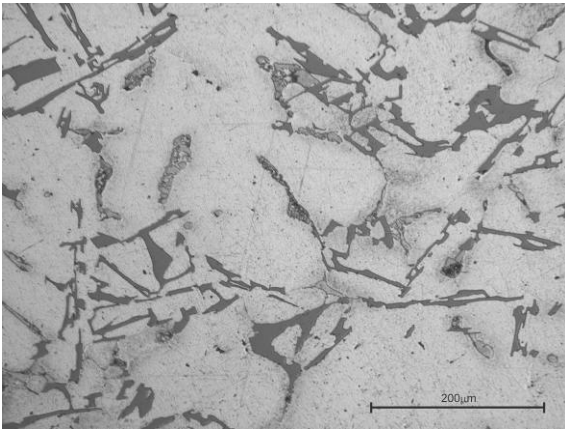
Fig. 3. Optical micrograph of the Al alloy, cylindrical sample of the A type, cooling rate 0.2ºC/s, plane parallel to the sample axis
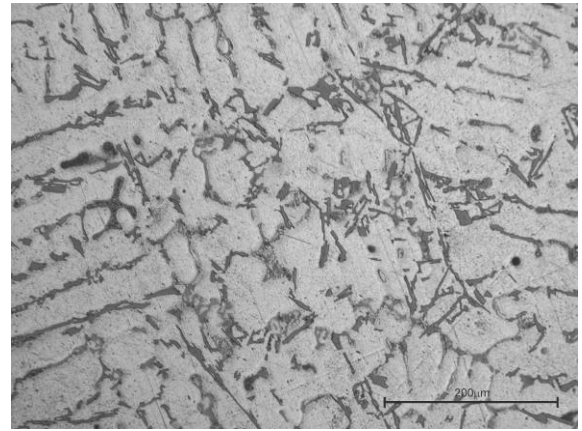

Fig. 6. Optical micrograph of the Al alloy, cylindrical sample of the A type, cooling rate 1°C/s, plane perpendicular to the sample axis
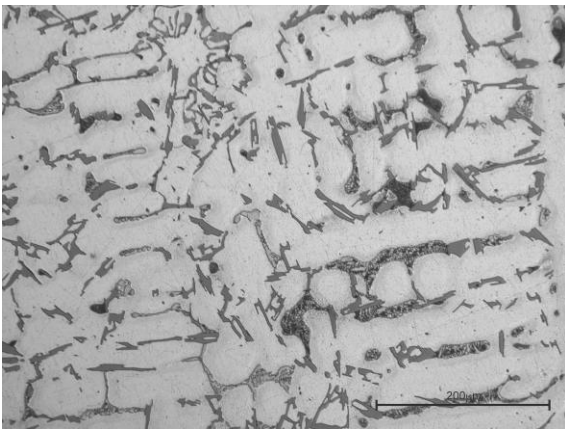

Fig. 4. Optical micrograph of the Al alloy, cylindrical sample of the A type, cooling rate 0.5°C/s, plane perpendicular to the sample axis
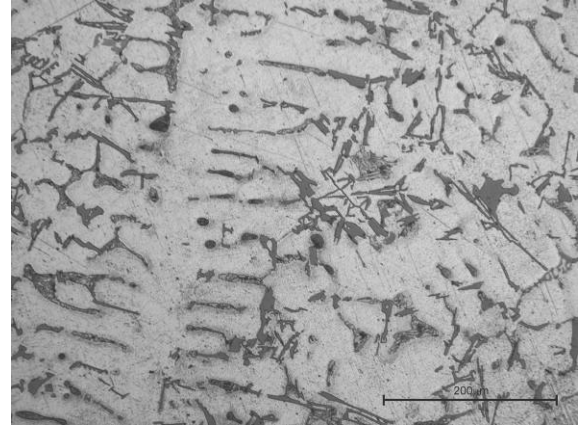

Fig. 7. Optical micrograph of the Al alloy, cylindrical sample of the A type, cooling rate 1ºC/s, plane parallel to the sample axis
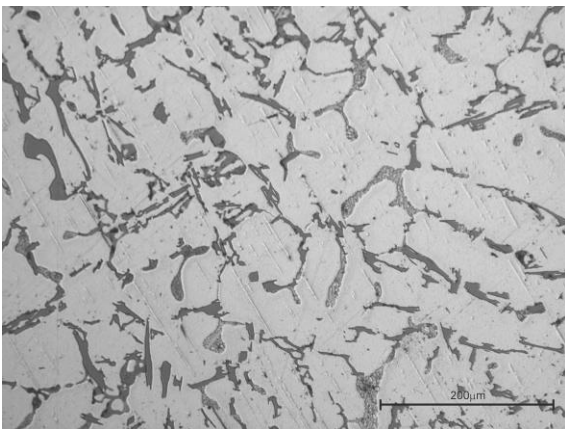

Fig. 5. Optical micrograph of the Al alloy, cylindrical sample of the A type, cooling rate 0.5°C/s, plane parallel to the sample axis
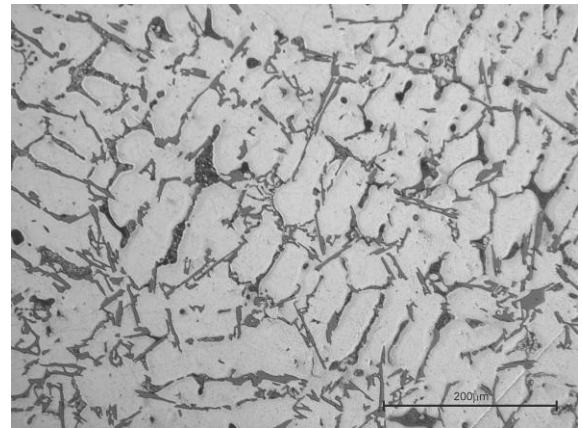

Fig. 8. Optical micrograph of the Al alloy, cylindrical sample of the A type, cooling rate 1.25°C/s, plane perpendicular to the sample axis
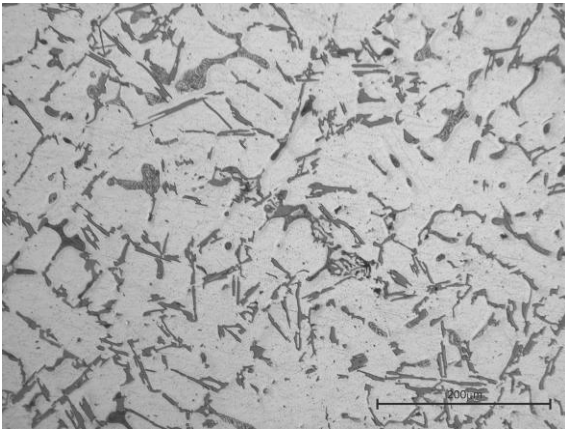
Fig. 9. Optical micrograph of the Al alloy, cylindrical sample of the A type, cooling rate 1.25°C/s, plane parallel to the sample axis
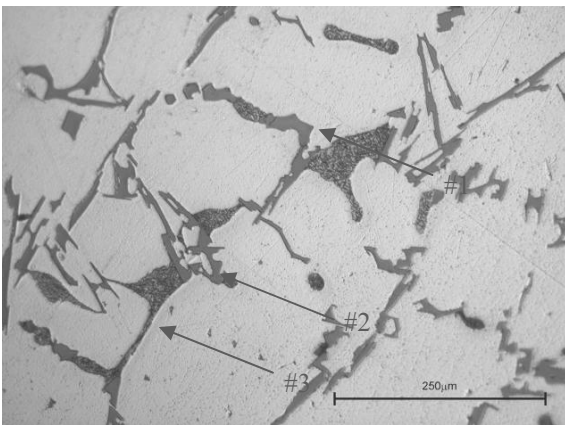

Fig. 10. Optical micrograph of the AlSi7Cu3Mg cooling rate 1°C/s with marked phases analysed in the work:1-$Al_{15}(MnFe)_3Si_2$, 2-Si, 3-Al_2Cu
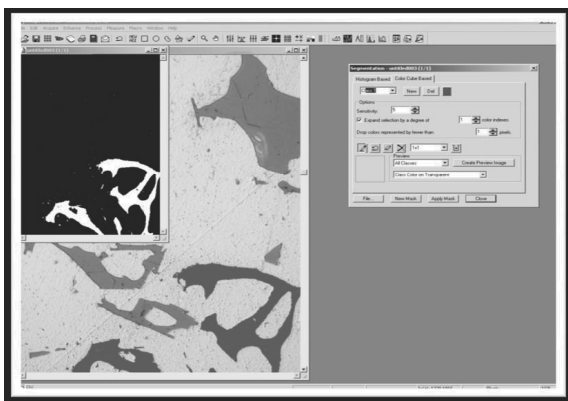

Fig. 11. Analysis of the $Al_{15}(MnFe)_3Si_2$ phase precipitations together with the generated matrix

As a result of the computer analysis of the metallographic structures for the AlSi7Cu3Mg alloy there was observed among others a slightly decrease (about 1%) of the percent α phase occurrence as well phase morphology change according to the cooling rate increase. The percent phase distribution is presented in Fig. 12. With increase of the cooling rate there occurs also an refinement of the α phase. For the Al_2Cu phase an increase of ca. 2% was observed, what is connected to Cu resolving in the Al matrix. On the basis of the performed investigations it can be conclude, that there is a lack of cooling rate influence in the range of 0.2-1°C/s on the percentage presence of the phases present in the microstructure, this is caused by the stability of the thermodynamic system.
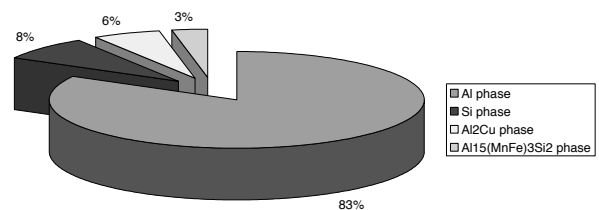

Fig. 12. Percent phase distribution for the 1.25°C/s cooling rate

However the cooling rate change in this range causes a microstructure refinement, what is presented on the diagram showing an average perimeter to surface ratio of the analysed phases occurred in the Al-Si-Cu alloy (Fig. 13).
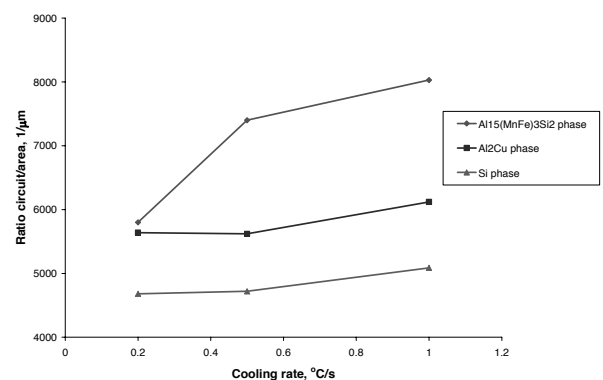
Fig. 13. Average value of the analyzed precipitation perimeter for the 0X and 0Y plane vs. the average surface area in comparison to the cooling rate of the investigated alloy

Percentage amount of pores in the samples increases together with the cooling rate, this dependence is also valid for cylindrical samples, which were cooled with the rates of 0.2°C/s, 0.5°C/s, 1°C/s.

Whereas for hollow cylindrical samples, cooled with 1.25°C/s, there occurs an decrease of the pores amount in comparison to the cylindrical samples cooled with the rate of 1°C/s (Fig. 14).

M. Krupiński, K. Labisz, L.A. Dobrzański, Z. Rdzawski

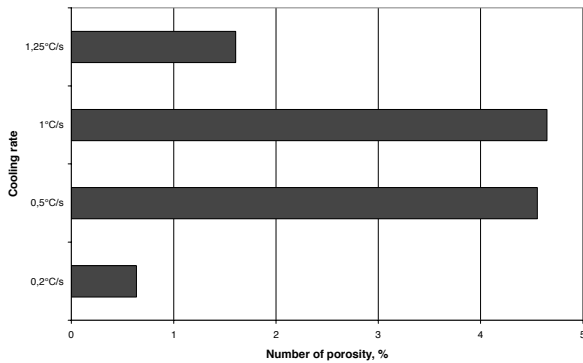Fig. 14. Percentage pores amount in the AlSi7Cu3Mg alloy in comparison to the cooling rate.

The differences in investigation results both for the phase and pores amount in case of the cylindrical sample can be dependent on the cooling way, where the sample was cooled not only from outside but also from inside simultaneously, what has influences the heat volume of the sample system.

In case of the percentage phase amount for the investigated microstructure micrographs there can be made following conclusions, that a significant importance for image analysis has the choice of the sample place chosen for measuring, as well

the distance from cooling surface, because the morphology itself is highly dependent on the place from where it was take for investigations. While the quality of the metallographic sample (scratches, surface roughness, etching) is of very big importance for the computer image analysis of the metallographic microstructure.

The major difficulties with the computer analysis were occurred in case of the α phase as well the $Al_{15}(MnFe)_3Si_2$ phase for the reason of the mutual overlaying histograms of the phase colours; in case of the Al_2Cu the major difficulty was connected to the phase morphology.

Analyzing the crystallisation process (Fig. 15) on the basis of the cooling curves is was state that at the T_L temperature starts the nucleation process of the α phase dendrites. On the derivative curve it is visible as a small inflexion point marked as *I, A, 1*, as well a temporary decrease in the cooling rate of the alloy. Heat effect accomplished to the nucleation process provide additionally heat to the remaining melt, however heat balance of the crystllised ingot is negative. The heat provided by the nuclei of the α phase is disproportional smaller compared to the heat give up to the surrounding through the cooled metal and causes only cooling rate decrease of the remaining melt. This process is going until the minimum of the crystallisation temperature of the dendrite α phase (point *II, B, 2* in the curves) is achieved, where the created nuclei achieves the critical value and the growing process of the α phase dendrite crystals is beginning.
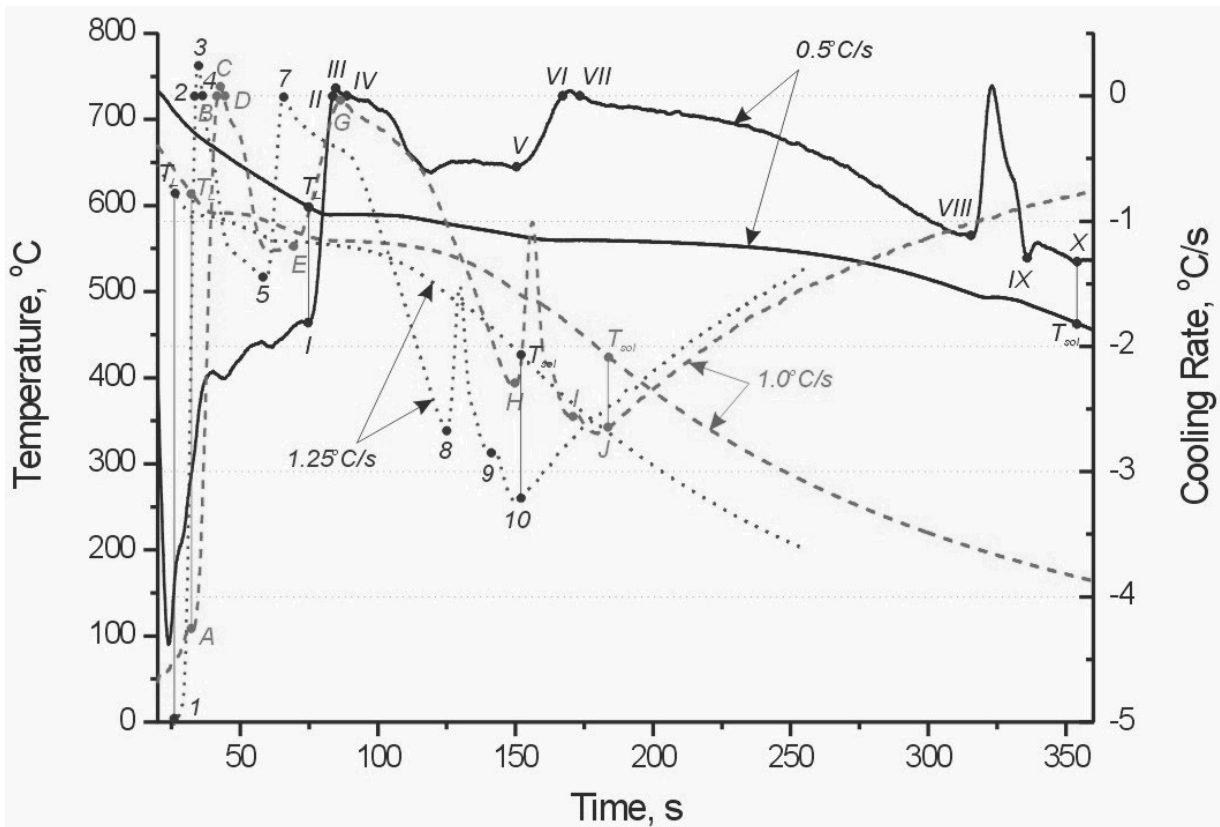

Fig. 15. Cooling curve and crystallisation curve of the AC-AlSi7Cu3Mg alloy cooled with different cooling rate: 1.25°C/s, 1°C/s, 0.5°C/s

The differential curves in this point takes zero as value. The crystallisation heat warms up the remaining melt to the temperature at point *III, C, 3*, where the created and freely growing crystals of the dendritic α phase begin to touch each others with some surfaces include the remaining melt inside. Next growth of the crystals causes a temperature increase of the melt to the maximal temperature value of the crystllised α phase, (point *IV, D, 4*), at this moment also the iron, manganese and silicon containing phase crystallisation occurs, what is confirmed in the literature [1]. The chemical composition of the remained melt changes according to the liquidus line in the Al–Si equilibrium diagram. The melt is enriched with Si and after the temperature at point *V, E, 5* is achieved the nucleation of the α+β eutectic begins. The temperature grows to the maximal crystallisation temperature of the eutectic (point *VII, G, 7*), where the spontaneous precipitation of the durable α i β phases occurs. Next undercooling of the melt causes the crystallisation of the multiphase eutectic Cu and Mg and α+β, which emit additive crystallisation heat, this is shown on the differential curve in form of clearly heat effects (point *VIII, H, 8* and *IX, I, 9*). The crystallisation ends after the T_{Sol} solidus temperature is achieved (point *X, J, 10*).

Description of the characteristic points on the cooling curve is shown in Table 2.

Table 2.
Description of the characteristic points on the cooling curve from Fig. 15

Point on the graph	Description
I, A, 1	T_L nucleation temperature
II, B, 2	Point of the beginning of the crystal growth (α phase dendrites)
III, C, 3	Point of the dendrites (α phase) growth
IV, D, 4	Point of the α phase dendrite growth and (Al+Fe+Mn+Si) precipitation growth
V, E, 5	Nucleation point of the α+β eutectic
VI	Point of the α+β eutectics growth
VII, G, 7	Point of the stable eutectic growth α+β, in this point occurs the thermal equilibrium of the crystallized phases
VIII, H, 8	Crystallization Point of Cμ, Mg and α+β eutectic
IX, I, 9	Endpoint of crystallization of Mg, Cu and α+β eutectic
X, J, 10	T_{Sol} temperature of the crystallization end

4. Conclusions

The phase morphology changes increase in relation to the cooling rate for the investigated Al-Si-Cu alloy. The higher cooling rate, the higher the refinement and dispersion of the phases (α, $Al_{15}(Fe,Mn)_3Si_2$ and Al_2Cu) present in the α matrix. Increase of the cooling rate (0.2°C/s-1°C/s) influences also the shape of the intermetallic phases. They are more elongated, needle like shaped (β phase), more dispersive as well less regular

(Al_2Cu phase) and fine grained ($Al_{15}(MnFe)_3Si_2$). For lower cooling rates, they more often are of a globular shape e.g. dendritic for the $Al_{15}(MnFe)_3Si_2$ phase. The amount of the pores increases together with the cooling rate, this dependence is valid also for cylindrical samples, which were cooled with the rates of 0.2°C/s; 0.5°C/s; 1°C/s.

Additional information

Selected issues related to this paper are planned to be presented at the 16th International Scientific Conference on Contemporary Achievements in Mechanics, Manufacturing and Materials Science CAM3S'2010 celebrating 65 years of the tradition of Materials Engineering in Silesia, Poland and the 13th International Symposium Materials IMSP'2010, Denizli, Turkey.

References

[1] L. Bäckerud, G. Chai, J. Tamminen, Solidification Characteristics of Aluminum Alloys, AFS, 1992.

[2] L.A. Dobrzański, R. Maniara, J.H. Sokolowski, The effect of cast Al-Si-Cu alloy solidification rate on alloy thermal characteristics, Journal of Achievements in Materials and Manufacturing Engineering 17 (2006) 217-220.

[3] J. Szajnar, T. Wróbel, Methods of inoculation of pure aluminium structure, Journal of Achievements in Materials and Manufacturing Engineering 27/1 (2008) 95-98.

[4] H. Yamagata, W. Kasprzak, M. Aniolek, H. Kurita, J.H. Sokolowski, The effect of average cooling rates on the microstructure of the Al-20% Si high pressure die casting alloy used for monolithic cylinder blocks, Journal of Materials Processing Technology 203 (2008) 333-341.

[5] J.P. Anson, J.E. Gruzleski, The quantitative discrimination between shrinkage and gas microporosity in cast aluminum alloys using spatial data analysis, Materials Characterization 43 (1999) 319-335.

[6] P.D. Lee, A. Chirazi, R.C. Atwood, W. Wan, Multiscale modelling of solidification microstructures, including microsegregation and microporosity, in an Al-Si-Cu alloy, Materials Science and Engineering A 365 (2004) 57-65.

[7] D.G. Prakash, B. Prasanna, D. Regener, Computational microstructure analyzing technique for quantitative characterization of shrinkage and gas pores in pressure die cast AZ91 magnesium alloys, Computational Materials Science 32 (2005) 480-488.

[8] L. Wojnar, K.J. Kurzydłowski, J. Szala, Practice of image analysis, PTS, Cracow, 2002 (in Polish).

[9] W.T. Kierkus, J.H. Sokolowski, Recent Advances in Cooling Curve Analysis: A New Method for determining the 'Base Line' Equation, AFS Transactions 66 (1999) 161-167.

[10] L.J. Yang, The effect of casting temperature on the properties of squeeze cast aluminium and zinc alloys, Journal of Materials Processing Technology 140 (2003) 391-396.

[11] Y.H. Zhu, Phase transformations of eutectoid Zn-Al alloys, Journal of Materials Science 36 (2001) 3973-3980.

M. Krupiński, K. Labisz, L.A. Dobrzański, Z. Rdzawski

[12] B. Krupińska, L.A. Dobrzański, Z. Rdzawski, K. Labisz, Cooling rate influence on microstructure of the Zn-Al cast alloy, Journal of Achievements in Materials and Manufacturing Engineering 38/2 (2010)115-122.

[13] E.M. da Costa, C.E. da Costa, F. Dalla Vecchia, C. Rick, M. Scherer, C.A. dos Santos, B.A. Dedavid, Study of the influence of copper and magnesium additions on the microstructure formation of Zn-Al hypoeutectic alloys, Journal of Alloys and Compounds 488/1 (2009) 89-99.

[14] E. Fraś, Alloys crystallisation, WNT, Warsaw, 2003 (in Polish).

[15] J. Sobczak, Innovations in foundry, Part 1, Institute of Foundry, Cracow, 2007 (in Polish).

[16] A.A Prensyakov, Y.A Gorban, V.V Chervyakova, The aluminium – zinc phase diagram, Russian Journal of Physical Chemistry 6 (1961) 632-633.

[17] B.K. Prasad, O.P. Modi, Slurry wear characteristics of zinc-based alloys: Effects of sand content of slurry, silicon addition to alloy system and traversal distance, Transactions of Nonferrous Metals Society of China 19/2 (2009) 277-286.

[18] R. MacKay, M. Djurdjevic, J.H. Sokolowski, The Effect of Cooling Rate on the Fraction Solid of the Metallurgical Reaction in the 319 Alloy, AFS Transactions 25 (2000) 521-529.

[19] L.A. Dobrzański, M. Krupiński, K. Labisz, Derivative thermo analysis of the near eutectic Al-Si-Cu alloy, Archives of Foundry Engineering 8/4 (2008) 37-40.

[20] M. Krupiński, K. Labisz, L.A. Dobrzański, Z. Rdzawski, Derivative thermo analysis of the Al-Si cast alloy with addition of rare earths metals, Archives of Foundry Engineering 10/1 (2010) 79-82.